Concentration and characterization of organic colloids in deep granitic groundwater using nanofiltration membranes for evaluating radionuclide transport

Daisuke Aosai[a], Daisuke Saeki[a], Teruki Iwatsuki[b], Hideto Matsuyama[a,*]

[a] Center for Membrane and Film Technology, Department of Chemical Science and Engineering, Kobe University, 1-1 Rokkodai, Nada, Kobe 657-8501, Japan

[b] Japan Atomic Energy Agency, 1-64 Yamanouchi Akeyo, Mizunami, 509-6132, Japan

*Corresponding author.

E-mail address: matuyama@kobe-u.ac.jp (H. Matsuyama).

Abstract

Understanding the properties of organic colloids is important for geological disposal of high-level radioactive waste in terms of radionuclide transport. To analyze organic colloids in deep groundwater, concentration techniques using adsorption resins and reverse osmosis (RO) membranes have been widely applied, because their concentrations in deep groundwater are very low and detection of the organic colloids in raw groundwater is difficult. However, these techniques have respective disadvantages such as chemical disturbance and membrane fouling caused by cations. To overcome their disadvantages, we propose a new concentration method using nanofiltration (NF) membranes to concentrate organic colloids rapidly without chemical disturbance and to selectively remove monovalent and divalent ions, which may cause inorganic and/or organic fouling. Concentration performance of the NF and RO membranes for aqueous solutions for humic acids was evaluated using a laboratory-scale membrane test unit. The time course of permeate flux and concentration of humic acids were measured. These membranes were applied to the concentration of actual groundwater obtained at a depth of 300 m at the Mizunami Underground Research Laboratory in Japan. The permeate flux and concentration of major ions and organic colloids were measured. The organic colloids concentrated by the NF membrane were successfully analyzed using pyrolysis gas chromatography coupled with mass spectrometry (Py-GC/MS) owing to their high concentrations and low concentrations of salts. The NF membrane was useful for the concentration of organic colloids and rare earth elements (REEs) in deep groundwater, and the findings of the organic colloid structures revealed by Py-GC/MS provided valuable information for evaluating the effect of organic colloids on radionuclide transport.

Keywords

Concentration, Nanofiltration membrane, Organic colloid, Groundwater, Radionuclide transport

1. Introduction

Colloids, such as particles and macromolecules ranging from 1 to 1000 nm in size, are widespread in various natural water sources [1]. Groundwater contains inorganic colloids, such as fragments of rock and clay minerals from dissolution and precipitation of the rock, and organic colloids such as humic substances [2-5]. Additionally, it has been clearly shown that the migration velocity of radionuclides can either increase or decrease in the presence of colloids [6-11]. Therefore, investigation of the physicochemical properties (e.g., concentration, size, shape, and chemical composition) of colloids is of great importance for geological disposal of high-level radioactive waste (HLW). In particular, the detailed structures of organic colloids, which have more complex structures than inorganic colloids, are not yet well understood.

Organic colloids, most of which are humic substances, are metabolized through natural or biological degradation, and involve mainly aromatic carbon and carboxyl groups [12-15]. Organic colloids have negative charges in their internal structures and adsorb radionuclides in groundwater. Although field investigations have been conducted to understand the effect of organic colloids on radionuclide transport [16,17], precise analysis of organic colloids in groundwater is difficult owing to their low concentrations [18,19]. To solve this issue, groundwater concentration techniques using adsorption resins [20,21] and reverse osmosis (RO) membranes [22,23] have been attempted. Although the method using adsorption resins concentrates samples into disproportionately enriched organic colloids, the samples are exposed to severe chemical conditions, resulting in chemical or physicochemical changes of the organic colloids. The method using RO membranes can concentrate organic colloids highly efficiently and rapidly without strong chemical exposure. However, this method requires sample pretreatment using a cation exchange resin to remove cations that cause precipitation onto the

membrane surface [22,23]. This pretreatment using a cation exchange resin affects the composition of rare earth elements (REEs) in the sample, which are regarded as analogues of trivalent actinides [24] and are important for HLW analysis.

In this study, we propose a novel concentration method using nanofiltration (NF) membranes, which can be operated rapidly without chemical disturbance, and does not require additional sample treatment such as cation exchange. NF membranes are generally looser than RO membranes [25]. Typically, monovalent ion rejection of NF membranes is not very high, while multivalent ions can be rejected at high levels. First, an aqueous solution of commercial humic acid was concentrated as a model of organic colloids using two types of NF membranes and an RO membrane. The recovery yield of humic acid was measured using a UV-vis spectrophotometer. Then, we sampled groundwater in granite at a depth of 300 m and concentrated the groundwater using the membranes. To confirm the applicability of this method for groundwater, concentrations of cations and anions in both the concentrate and permeate water were measured by ion chromatography (IC). To characterize the chemical structures of the concentrated organic colloids, the concentrate water was analyzed by pyrolysis gas chromatography coupled with mass spectrometry (Py-GC/MS). Py-GC/MS is commonly used to obtain detailed structural information on the components of natural organic matter, although salt removal is required [26]. Moreover, REE concentrations in the concentrated groundwater enriched by the two types of NF membranes and the RO membrane were measured by inductively coupled plasma mass spectrometry (ICP-MS).

2. Materials and methods

2.1 Materials for performance evaluation of NF and RO membranes

Two types of commercial NF membranes (NTR7410 and NTR7450; Nitto Denko, Osaka, Japan) composed of sulfonated polyethersulfone and a commercial RO membrane (ES20; Nitto Denko, Osaka, Japan) composed of aromatic polyamide were used. All solutions used in this study were prepared using ultrapure water and analytical-grade chemicals. Humic acid derived from peat (H16752; Sigma-Aldrich, St. Louis, MO, USA) was used after the following pretreatment process. The humic acid was dissolved in a NaOH solution (pH 10) and the pH was adjusted to 1 with a HCl solution to remove fulvic acid and heavy metals. The sample was centrifuged to remove ash, and then the residue was freeze-dried. The elemental composition of this humic acid has been previously reported: 55.5% C, 38.9% O, 4.6% H, and 0.6% N [27]. This humic acid has been used extensively as a model organic colloid by many researchers [28-31] owing to its easy availability and well-characterized properties.

2.2 Groundwater sampling

Groundwater was collected from the 09MI20 borehole in the −300 m access/research gallery of Mizunami Underground Research Laboratory (MIU) on December 25, 2014. The Miocene sedimentary rocks (Mizunami Group) unconformably overlie the Cretaceous granitic rocks (Toki granite) at a depth of ~160 m at the MIU site. The groundwater in the granite was weakly alkaline Na–(Ca)–Cl-type, and the salinity increased with depth as a result of mixing of deeply lying saline water with recharged meteoric water [32]. The 09MI20 borehole is a horizontal borehole with a length of 102 m and was designed for investigations of hydrochemical changes related to facility construction. The borehole is divided into six sections by impermeable packers and the sections are numbered from 1 to 6 according to the distance from the base of the borehole. Groundwater samples were collected from section 1. Hydrochemistry of the

groundwater is summarized in Table 1.

2.3 Concentration apparatus

A laboratory-scale cross-flow concentration apparatus was used to concentrate aqueous solutions (Fig. 1) [33]. A feed solution was fed into a membrane cell using a plunger pump (NPL-120; Nihon Seimitsu Kagaku Co., Tokyo, Japan) with a constant flow rate of 9.0 mL/min. The applied pressure was maintained at 1.5 MPa using a back pressure valve. The effective area of sample membranes was 8.0 cm^2. The permeate solution was collected in a permeate reservoir. The feed solution was recycled into the feed reservoir and was concentrated from 500 mL to a minimum of 25 mL. The feed solution side of the membrane cell was magnetically stirred at 150 rpm. The permeate flux was calculated from the weight gain.

2.4 Concentration test of humic acid

A feed solution of 1 mg/L of humic acid was used. The recovery yield was evaluated through the concentration ratio of humic acid in the feed solution before and after the concentration test. The concentration of the humic acid was measured using a UV-vis spectrometer at 254 nm (V-650; Jasco Corp., Tokyo, Japan).

2.5 Concentration of groundwater

The groundwater was concentrated from 500 mL to 25 mL using the NF membranes (NTR7410, NTR7450) and from 500 mL to 80 mL using the RO membrane (ES20). Organic colloid concentration was calculated on the assumption that all organic colloids were humic acid. The recovery yield of organic colloids was evaluated by using the organic colloid concentrations

in the concentrated solution and raw solution. Cationic species (Na^+, K^+, Ca^{2+}) and anionic species (F^-, Cl^-, SO_4^{2-}) in the concentrate and permeate water of the groundwater were analyzed by ion chromatography (ICS-3000; Dionex Corp., Sunnyvale, CA, USA). For cation separations, an IonPac CS16 (250 × 5 mm, Dionex Corp.) analytical column and IonPac CG16 (50 × 5 mm, Dionex Corp.) guard column were used, and the eluent was CH_3SO_3H. For anion separations, an IonPac AS18 (250 × 4 mm, Dionex Corp.) analytical column and IonPac AG18 (50 × 4 mm, Dionex Corp.) guard column were used, and the eluent was KOH. REE concentrations in the raw and concentrated groundwater were measured by ICP-MS (Agilent 7000x; Agilent Technologies Inc., Palo Alto, CA, USA). The REE isotopes monitored with ICP-MS were ^{139}La, ^{140}Ce, ^{141}Pr, ^{146}Nd, ^{149}Sm, ^{151}Eu, ^{157}Gd, ^{159}Tb, ^{163}Dy, ^{165}Ho, ^{166}Er, ^{169}Tm, ^{172}Yb, and ^{175}Lu. The calibration curves were constructed from 1, 5, 10, 50, 100, and 500 ng/L REE solutions prepared from a 10 mg/L REE standard solution (SPEX CertiPrep Ltd., London, UK). The detection limit values of the REEs were 1 ng/L. After concentration of the groundwater, membranes were dried and analyzed by attenuated total reflectance Fourier transform infrared spectroscopy (ATR-FTIR). These measurements were carried out using a Nicolet iS5 FT-IR spectrometer with an iD5 diamond advanced attenuated total reflectance attachment (Thermo Fisher Scientific, Waltham, MA, USA).

2.6 Characterization of concentrated organic colloids

The groundwater concentrated by NF7450 was further evaporated, dried under N_2, and analyzed by Py-GC/MS. The Py-GC/MS analysis was performed using a double-shot pyrolyzer (PY-2020id; Frontier Laboratories Ltd., Fukushima, Japan) attached to a GC/MS instrument (Agilent 6890N/Agilent 5973; Agilent Technologies Inc., Palo Alto, CA, USA) with a DB-5ms

fused silica column (30 m × 0.25 mm i.d. × 0.25 μm film thickness, Agilent Technologies Inc.). The sample was heated at 600 °C for 1 min, and the evolved gases were then directly injected into the GC/MS instrument for analysis. Helium was used as a carrier gas at a constant flow of 1 mL/min. The column temperature was programmed from 40 to 300 °C at 10 °C/min and held at 300 °C for 15 min. The mass spectrometer was operated in electron impact ionization mode with an ionizing energy of 70 eV. Compound identification was based on comparisons of the mass spectra and relative retention times with those in the NIST and Wiley library databases.

3. Results and discussion

3.1 Concentration of model humic acid

Fig. 2 shows the time courses of the permeate flux and humic acid concentration in the concentrated solutions in the concentration tests using the three types of membranes (NTR7410, NTR7450, and ES20). In this figure, the calculated concentrations in the concentrated solutions with 100% recovery yield are plotted as dotted lines. Fig. 3 shows the relationship between the humic acid concentration in the concentrated solution and the concentration magnification. The concentration magnification is defined as the volume of the raw solution divided by that of the concentrated solution. The dotted lines in these figures show the calculated relationships in the case of 100% recovery yield. The concentration test using NTR7410 showed the highest initial permeate flux followed by an immediate decrease (Fig. 2a and 3a). The humic acid concentrations in concentrated solutions were below the dotted line, indicating low recovery yields. The recovery yield at 20-fold concentration was only 26%. The decrease in the permeate flux and the low recovery yield were probably due to the membrane fouling caused by humic acid. Large amounts of the humic acids were adsorbed on the membrane surface and reduced the water permeation. On the other hand, the water flux hardly decreased throughout the

concentration test using NTR7450, and the recovery yield of humic acid at 20-fold concentration was as high as 81% (Fig. 2b and 3b). Although the two membranes are basically composed of the same material, sulfonated polyethersulfone, the tendencies of the flux changes were clearly different, suggesting that the high initial flux causes severe flux decline and low recovery yield of humic acid. This result is consistent with those of previous studies [29-31,33], which reported that humic acid fouls membranes via a hydrodynamic drag force caused by the water flux toward a membrane surface. The concentration using ES20 hardly showed a permeate flux decrease and achieved the highest recovery yield of 90% at 20-fold concentration (Fig. 2c and 3c). Although the initial fluxes of NTR7450 and ES20 were similar, the difference in the membrane materials, sulfonated polyethersulfone of NTR7450 and aromatic polyamide of ES20, probably affected the membrane fouling by humic acid.

3.2 Concentration of groundwater

3.2.1 Concentration of organic colloids in groundwater

Fig. 4 shows the time courses of the permeate flux and organic colloid concentration in the concentrated solutions in the groundwater test. Fig. 5 shows the relationship between the organic colloid concentration in the concentrated solution and the concentration magnification. The permeate flux of NTR7410 decreased slightly throughout the concentration test, and the recovery yield of the organic colloids at 20-fold concentration was only 8.8% (Fig. 4a and 5a). The permeate flux decline and low recovery yield were considered to be due to organic colloid fouling, similar to the case of the humic acid experiment. In the case of using NTR7450, the recovery yield at 20-fold concentration was 57%, and the initial permeate flux was maintained throughout the concentration test (Fig. 4b and 5b). In the case of using ES20, the permeate flux

was constant for approximately 300 min, and then declined suddenly over the twofold concentration (Fig. 4c and 5c). Therefore, it was difficult to concentrate the solution to more than 6-fold concentration. This drastic decline in the permeate flux did not occur in the concentration test of model humic acid. Therefore, it is suggested that inorganic substances in the groundwater precipitate on the membrane surface and bring about the permeate flux decline. This will be discussed in section 3.2.2.

3.2.2 Effect of inorganic substances on concentration of organic colloids

To understand the effect of the inorganic substances on the recovery yield of the organic colloids and the decline of the permeate flux, the concentrations of major ions Na^+, K^+, Ca^{2+}, Cl^-, F^-, and SO_4^{2-} in both the concentrated and permeate solutions from the groundwater were measured. As shown in Table 1, since the major components of the groundwater were Na^+, K^+, Ca^{2+}, Cl^-, F^-, and SO_4^{2-}, we measured these ion concentrations. Fig. 6 shows the relationship between the cation concentrations in both the concentrated and the permeate solutions and the concentration magnification in the concentration tests using the three types of membranes. Fig. 7 shows the results of the anions. The dotted lines in both figures represent the calculated concentrations in the case of 100% recovery yield. In the case of using NTR7410, the concentrations of all ions in the permeate solution and concentrated solution were approximately equal, suggesting that these ions were not rejected by this membrane (Fig. 6a and 7a). In the NTR7450 test, although the concentrations of monovalent ions in the permeate solution were slightly lower than those in the concentrated solution, the concentrations of Ca^{2+} and SO_4^{2-} increased more than those of monovalent ions (Fig. 6b and 7b). On the other hand, for ES20, most ions were not detected in the permeate solution and recovery yields were almost 100%

except for Ca^{2+} and F^{-} in the regions of high concentration magnification (Fig. 6c and 7c). This result indicates that Ca^{2+} and F^{-} may form less-soluble salts such as $CaCO_3$ and CaF_2, and precipitated on the membranes when the concentrations exceeded the supersaturation values.

The FTIR spectra of the membrane surfaces after the concentration test are shown in Fig. 8. A strong broad band at 1400 cm^{-1} was observed in the FTIR spectrum of ES20, but not in the spectra of NTR7410 and NTR 7450. The strong broad band was generally attributed to CO_3 [34]. This result indicates that $CaCO_3$ precipitated on ES20. However, it was difficult to confirm the precipitation of CaF_2, because CaF_2 shows no band. A previous study reported that less-soluble salts were supersaturated by membrane concentration, precipitated on the membrane surface, and blocked the membrane pore [22,23]. Moreover, the high calcium concentration induces severe membrane fouling in the presence of humic acid. Increasing calcium concentrations significantly reduces negative net charges of humic acids [27,29-31,35], resulting in a more compact, energetically stable conformation [35,36]. In addition, Ca^{2+} ions bridge humic acid molecules [37]. Thus, the bridged humic acid molecules caused by the increased Ca^{2+} concentration accelerated the membrane fouling. Therefore, in the concentration test using ES20 with high rejection properties, it is suspected that Ca^{2+} was concentrated over the supersaturation value by concentration polarization and precipitated on the membrane surfaces, resulting in the sudden flux decrease shown in Fig. 4c.

3.2.3 Applicability of NF and RO membranes for concentration of organic colloids

As shown in Fig. 5, organic colloids were concentrated from 0.4 mg/L to 1.7 mg/L using ES20. However, it was difficult to concentrate further owing to the precipitation of the concentrated inorganic substances on the membrane surfaces and the fouling of the organic colloids caused by

concentrated Ca^{2+}. In the case of using NTR7410, organic colloids were only concentrated from 0.4 mg/L to 0.7 mg/L owing to organic fouling caused by the high initial permeate flux. In the case of using NTR7450, the organic colloids were concentrated from 0.4 mg/L to 4.6 mg/L with high recovery yield due to prevention of concentration polarization by removing ions. The NTR7450 membrane has high applicability for concentration of organic colloids in groundwater because of the moderate initial permeate flux and ion rejection.

3.2.4 Structure of organic colloids

The organic colloids in the concentrated groundwater samples were analyzed by Py-GC/MS. The samples concentrated by NTR7410 or ES20 were not applied to Py-GC/MS due to their low concentrations of organic colloids and/or high concentrations of salts. The Py-GC/MS pyrogram of the organic colloid in the groundwater concentrated by NTR7450 is presented in Fig. 9. More than 30 compounds were detected, which are listed in Table 2. Most of the compounds are the same as those detected in previous pyrolysis studies of humic substances from soil, peat, lignites, and aquatic sources [38-41]. The main pyrolysis compounds can be identified by source polymer such as carbohydrates, proteins, lignin, and lipids [42]. As shown in Fig. 9, pyrolysis compounds arising from carbohydrates such as furan and its derivatives were not detected, while trace amounts of N-containing compounds (n = 1, 10) arising from proteins were detected. Phenol (n = 10) and alkyl phenols (n = 14) arising from lignin-derived subunits in wood material [43,44] were weakly detected. The series of aliphatic compounds (n = 3, 7, 11, 16, 19, 21, 24, 26) arising from polymethylene structures such as lipids with long aliphatic chains and paraffinic material was detected, but relatively weakly. Thus, the major pyrolysis products of organic colloids were aromatic products. Lu et al. [42] reported that a high abundance of aromatic products indicates

high humification, and carbohydrates are lost during humification. Therefore, it is suspected that most parts of the organic colloid structures in deep groundwater were similar to humic substances with high humification. The concentration method using NTR7450 enabled the analysis of organic colloids in groundwater without adsorption resins or cation exchange, which affect the REE composition.

3.2.5 Concentration of REEs

For concentrated groundwater, the composition of REEs was measured. Table 3 shows the REE concentrations in the raw and concentrated groundwater in the concentration tests using the three types of membranes. Some REE concentrations in the groundwater concentrated by NTR7450 and ES20 could be detected by ICP-MS, while those in the raw groundwater were lower than the detection limit. Although the obtained REE concentrations were not very high, NTR7450 could concentrate the samples to much higher concentrations for a longer time for a more accurate analysis. Thus, this concentration method would be promising for concentrating organic colloids and REEs in groundwater efficiently and for understanding the interaction between organic colloids and REEs.

4. Conclusions

In this study, we applied NF and RO membranes to the concentration of organic colloids. Although the recovery yield using the RO membrane was high in the model humic acid concentration test, concentration of groundwater was difficult owing to the precipitation of inorganic substances on membranes and membrane fouling caused by organic colloids with Ca^{2+}. On the other hand, an NF membrane with moderate initial flux and ion rejection achieved

20-fold concentration of groundwater with 57% recovery yield of organic colloids. Based on the Py-GC/MS measurement of the concentrated groundwater, it is suspected that organic colloid structures in granite groundwater at a depth of 300 m are similar to those of humic substances with high humification. Thus, the groundwater concentration technique using NF membrane presented in this work could be a useful method to investigate the physicochemical properties of colloids in the groundwater.

Acknowledgments

We would like to thank Y. Amata, T. Okunomiya, and D. Soga (KOBELCO RESEARCH INSTITUTE) for the groundwater analyses.

References

[1] M. Filella, Colloidal properties of submicron particles in natural waters, in: K.J. Wilkinson, J.R. Lead (Eds.), Environmental Colloids and Particles: Behaviour, Separation and Characterization, Wiley, Chichester (2007) 17–94.

[2] D. Backhus, Sampling colloids and colloid-associated contaminants in groundwater, Ground Water 31 (1993) 466–479.

[3] P. Vilks, D.B. Bachinski, Characterization of organics in Whiteshell Research area groundwater and the implications for radionuclide transport, Appl. Geochem. 11 (1996) 387–402.

[4] T. Saito, Y. Suzuki, T. Mizuno, Size and elemental analyses of nano colloids in deep granitic groundwater: implications for transport of trace elements, Colloids Surf. A: Physicochem. Eng. Asp. 435 (2013) 48–55.

[5] D. Aosai, Y. Yamamoto, T. Mizuno, T. Ishigami, H. Matsuyama, Size and composition analyses of colloids in deep granitic groundwater using microfiltration/ultrafiltration while maintaining in situ hydrochemical conditions, Colloids and Surf. A: Physicochem. Eng. Asp. 461 (2014) 279–286.

[6] A.B. Kersting, D.W. Efurd, D.L. Finnegan, D.J. Rokop, D.K. Smith, J.L. Thompson, Migration of plutonium in ground water at the Nevada Test Site, Nature 397 (1999) 56–59.

[7] W.R. Penrose, W.L. Polzer, E.H. Essington, D.M. Nelson, K.A. Orlandini, Mobility of plutonium and americium through a shallow aquifer in a semiarid region, Environ. Sci. Technol. 24 (1990) 228–234.

[8] G.J. Moridis, Q. Hu, Y.S. Wu, G.S. Bodvarsson, Preliminary 3-D site-scale studies of radioactive colloid transport in the unsaturated zone at Yucca Mountain, Nevada, J. Contam. Hydrol. 60 (2003) 251–286.

[9] A.P. Novikov, S.N. Kalmykov, S. Utsunomiya, R.C. Ewing, F. Horreard, A. Merkulov, S.B. Clark, V.V. Tkachev, B.F. Myasoedov, Colloid transport of plutonium in the far-field of the Mayak Production Association, Russia, Science 314 (2006) 638–641.

[10] J.N. Ryan, M. Elimelech, Colloid mobilization and transport in groundwater, Colloids and Surf. A 107 (1996) 1–56.

[11] J.F. McCarthy, J.M. Zachara, Subsurface transport of contaminants, Environ. Sci. Technol. 23 (1989) 496–502.

[12] R. Artinger, G. Buckau, S. Geyer, P. Fritz, M. Wolf, J.I. Kim, Characterization of groundwater humic substances: influence of sedimentary organic carbon, Appl. Geochem. 15 (2000) 97–116.

[13] S.W. Krasner, J. Croue, J. Buffle, E.M. Perdue, Three approaches for characterizing NOM, J.

Am. Water Works Assoc. 88 (1996) 66–79.

[14] J.A. Leenheer, Systematic approaches to comprehensive analyses of natural organic matter, Ann. Environ. Sci. 3 (2009) 31–130.

[15] H.Z. Ma, H.E. Allen, Y.J. Yin, Characterization of isolated fractions of dissolved organic matter from natural waters and a wastewater effluent, Water Res. 35 (2001) 985–996.

[16] N.A. Marley, J.S. Gaffney, K.A. Orlandini, M.M. Cunningham, Evidence of radionuclide transport and mobilization in a shallow, sandy aquifer, Environ. Sci. Technol. 27 (1993) 2456–2461

[17] F. Caron, G. Mankarios, Pre-assessment of the speciation of ^{60}Co, ^{125}Sb, ^{137}Cs and ^{241}Am in a contaminated aquifer, J. Environ. Radioactivity 77 (2004) 29–46.

[18] J. Gaillardet, J. Viers, B. Dupré, Trace elements in river waters, in: J.I. Drever(Ed.), Treatise on Geochemistry, Elsevier, Amsterdam, (2003) 225–272.

[19] M. Plaschke, J. Romer, J.I. Kim, Characterization of Gorleben groundwater colloids by atomic force microscopy, Environ. Sci. Technol. 36 (2002) 4483–4488.

[20] E.M Thurman, R.L Malcom, Preparative isolation of aquatic humic substances, Environ. Sci. Technol. 15 (1981) 463–466.

[21] C.J. Miles, J.R. Tuschall Jr, P.L. Brezonik, Isolation of aquatic humus with diethylaminoethylcellulose. Anal. Chem., 55 (1983) 410–411.

[22] S.M. Serkiz, E.M. Perdue, Isolation of dissolved organic matter from the Suwannee River using reverse osmosis, Water Res. 24 (1990) 911–916.

[23] L. Sun, E.M. Perdue, J.F. McCarthy. Using reverse osmosis to obtain organic matter from surface and ground waters, Water Res. 29 (1995) 1471–1477.

[24] N. Chapman, J. Smellie, Introduction and summary of the workshop, Chem. Geol. 55

(1986) 167–173.

[25] S. Hong, M. Elimelech, Chemical and physical aspects of natural organic matter (NOM) fouling of nanofiltration membranes, J. Membr. Sci. 132 (1997) 159–181.

[26] H. Iwai, M. Fukushima, M. Yamamoto, T. Komai, Y. Kawabe, Characterization of seawater extractable organic matter from bark compost by TMAH-py-GC/MS, J. Anal. Appl. Pyrolysis 99 (2013) 9–15.

[27] M.J. Avena, L.K. Koopal, W.H. van Riemsdijk, Proton binding to humic acids: Electrostatic and intrinsic interactions. J. Colloid Interface Sci. 217 (1999) 37–48.

[28] W. Yuan, A.L. Zydney, Humic acid fouling during ultrafiltration. Environ. Sci. Technol. 34 (2000) 5043–5050.

[29] S.K. Hong, M. Elimelech, Chemical and physical aspects of natural organic matter (NOM) fouling of nanofiltration membranes. J. Membr. Sci. 132 (1997) 159–181.

[30] A. Seidel, M. Elimelech, Coupling between chemical and physical interactions in natural organic matter (NOM) fouling of nanofiltration membranes: implications for fouling control. J. Membr. Sci. 203 (2002) 245–255.

[31] C.Y. Tang, Y.N. Kwon, J.O. Leckie, Fouling of reverse osmosis and nanofiltration membranes by humic acid—effects of solution composition and hydrodynamic conditions, J. Membr. Sci. 290 (2007) 86–94.

[32] T. Iwatsuki, R. Furue, H. Mie, S. Ioka, T. Mizuno, Hydrochemical baseline condition of groundwater at the Mizunami underground research laboratory (MIU), Appl. Geochem. 20 (2005) 2283–2302.

[33] D. Saeki, T. Tanimoto, H. Matsuyama, Prevention of bacterial adhesion on polyamide reverse osmosis membranes via electrostatic interactions using a cationic phosphorylcholine

polymer coating, Colloids and Surf. A: Physicochem. Eng. Asp. 443 (2014) 171–176.

[34] F.A. Andersen, L. Brecevic, Infrared spectra of amorphous and crystalline calcium carbonate, Acta Chem. Scand. 45 (1991) 1018–1024.

[35] C.L. Tiller, C.R. Omelia, Natural organic matter and colloidal stability: Models and measurements, Colloids and Surf. A: Physicochem. Eng. Asp. 73 (1993) 89–102.

[36] K. Ghosh, M. Schnitzer, Macromolecular structures of humic substances, Soil Sci. 129 (1980) 266.

[37] F.J. Stevenson, Humus chemistry, John Wiley & Sons: New York, 1982.

[38] C. Sáiz-Jiménez, J.W. De Leeuw, Chemical characterization of soil organic matter fractions by analytical pyrolysis-gas chromatography-mass spectrometry, J. Anal. Appl. Pyrolysis 9 (1986) 99–119.

[39] J.A. González-Pérez, G. Almendros, J.M. de la Rosa, F.J. González-Vila, Appraisal of polycyclic aromatic hydrocarbons (PAHs) in environmental matrices by analytical pyrolysis (Py–GC/MS), J. Anal. Appl. Pyrolysis 109 (2014) 1–8.

[40] M.A. Wilson, R.P. Philp, A.H. Gillam, T.D. Gilbert, K.R. Tate, Comparison of the structures of humic substances from aquatic and terrestrial sources by pyrolysis gas chromatography-mass spectrometry, Geochim. Cosmochim. Acta 47 (1983) 497–502.

[41] R. Sihombing, P.F. Greenwood, M.A. Wilson, J.V. Hanna, Composition of size exclusion fractions of swamp water humic and fulvic acids as measured by solid state NMR and pyrolysis-gas chromatography-mass spectrometry, Org. Geochem. 24 (1996) 859–873.

[42] X.Q. Lu, J.V. Hanna, W.D. Johnson, Source indicators of humic substances: an elemental composition, solid state 13 C CP/MAS NMR and Py-GC/MS study, Appl. Geochem. 15 (2000) 1019–1033.

409 [43] F. Martin, C. Sáiz-Jiménez, F.J. GonzaÁlez-Vila, Pyrolysis-gas chromatography-mass
410 spectrometry of lignins, Holzforschung 33 (1979) 210–212.
411 [44] C. Sáiz-Jiménez, J.W. de Leeuw, Chemical structure of a soil humic acid as revealed by
412 analytical pyrolysis. J. Anal. Appl. Pyrolysis 11 (1987) 367–376.
413

414 Table 1 Hydrochemistry of groundwater sampled from 09MI20 borehole section 1 at a depth of 300 m on December 25, 2014.

pH	EC	Na^+	K^+	Ca^{2+}	Cl^-	F^-	SO_4^{2-}	Mg	Al	Fe	Mn	Dissolved inorganic carbon	Dissolved organic carbon	M-Alkalinity
	[mS/m]	[mg/L]	[mg/L]	[mg/L]	[mg/L]	[mg/L]	[mg/L]	[mg/L]	[mg/L]	[mg/L]	[mg/L]	[mg/L]	[mg/L]	[meq/L]
8.5	43	76	0.4	9.0	64	9.8	13	0.11	<0.01	<0.005	<0.003	13	<0.5	1.19

415

416

417 Table 2 Typical pyrolysis compounds of organic colloids in groundwater concentrated by NTR7450

Peak No.	Compound	Group
1	Pyrrole	N-containing
2	Toluene	Aromatic
3	Octene	Aliphatic carbon
4	Ethylbenzene	Aromatic
5	Xylene	Aromatic
6	Styrene	Aromatic
7	Nonene	Aliphatic carbon
8	C_3-Alkylbenzene	Aromatic
9	Methylstyrene	Aromatic
10	Phenol and Benzonitrile	Hydroxy benzene and N-containing
11	Decene and C_3-Alkylbenzene	Aliphatic carbon and aromatic
12	C_3-Alkylbenzene	Aromatic
13	Indene	Aromatic
14	Cresol	Hydroxy benzene
15	Methylbenzaldehyde	Aromatic
16	Undecene	Aliphatic carbon
17	C_4-Alkylbenzene	Aromatic
18	Naphthalene	Aromatic
19	Dodecene	Aliphatic carbon
20	C_5-Alkylbenzene	Aromatic
21	Tridecene	Aliphatic carbon
22	Methylnaphthalene	Aromatic
23	Biphenyl	Aromatic
24	Tetradecene	Aliphatic carbon
25	Methylbiphenyl or Dimethylnaphthalene	Aromatic

26	Pentadecene	Aliphatic carbon
27	Fluorene	Aromatic
28	Dihydrophenanthrene or Dihydroanthracene	Aromatic
29	Phenanthrene	Aromatic
30	Anthracene	Aromatic
31	Methylphenanthrene and Methylanthracene	Aromatic
32	Pyrene	Aromatic
33	Methylpyrene	Aromatic

418

419

420 Table 3 REE concentrations of raw and concentrated groundwater

	La [ng/L]	Ce [ng/L]	Pr [ng/L]	Nd [ng/L]	Sm [ng/L]	Eu [ng/L]	Gd [ng/L]	Tb [ng/L]	Dy [ng/L]	Ho [ng/L]	Er [ng/L]	Tm [ng/L]	Yb [ng/L]	Lu [ng/L]
Raw groundwater	<1	<1	<1	1	<1	<1	<1	<1	1	<1	2	<1	2	<1
20-fold concentrate (NTR7410)	1	2	<1	<1	<1	<1	<1	<1	<1	<1	<1	<1	<1	<1
20-fold concentrate (NTR7450)	<1	3	<1	2	<1	<1	<1	<1	1	<1	3	<1	5	2
6.25-fold concentrate (ES20)	<1	2	<1	3	<1	<1	1	<1	4	2	7	2	6	2

421

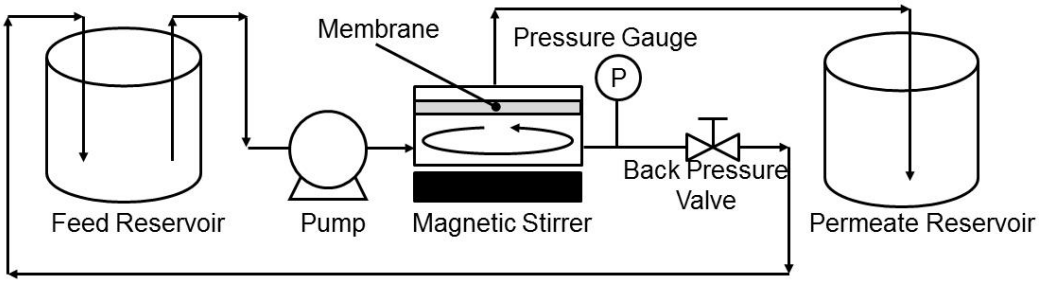

Fig. 1. Schematic diagram of the cross-flow concentration apparatus

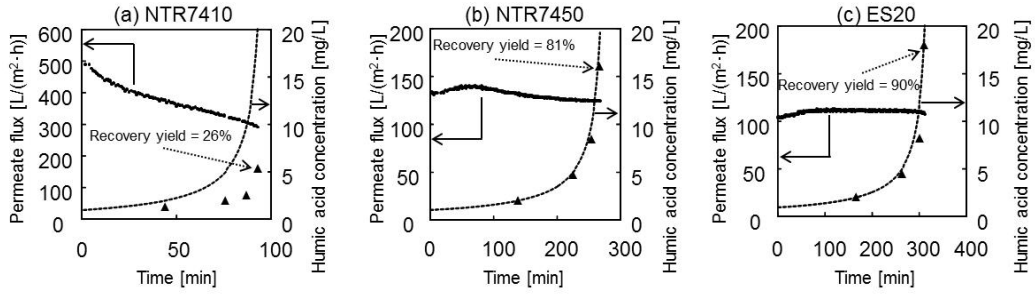

Fig. 2. Time courses of the permeate fluxes and humic acid concentrations in the concentrated solutions in the concentration tests of humic acid with (a) NTR7410, (b) NTR7450, and (c) ES20. Black circles and black triangles indicate permeate flux and humic acid concentration, respectively. Dotted lines indicate calculated concentrations if recovery yield = 100%.

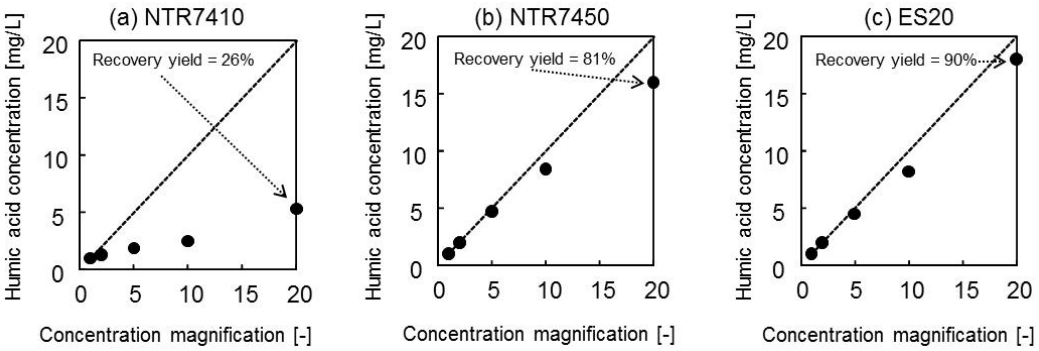

Fig. 3. Relationship between the humic acid concentration in the concentrated solution and the concentration magnification of (a) NTR7410, (b) NTR7450, and (c) ES20. Dotted lines indicate the calculated concentration if recovery yield = 100%.

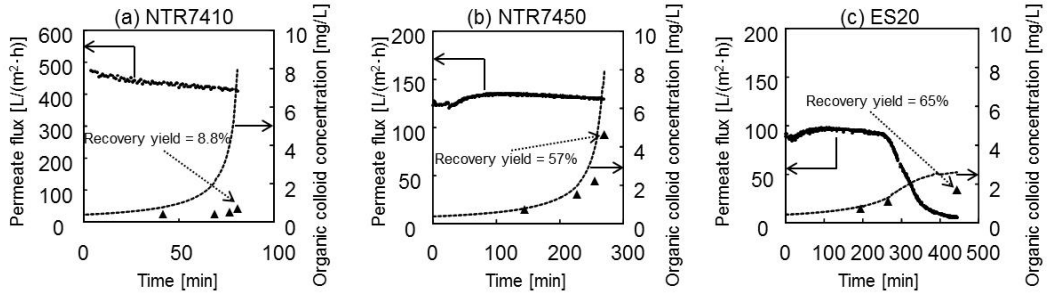

Fig. 4. Time courses of the permeate fluxes and organic colloid concentrations in the concentrated solutions in the concentration tests of the groundwater using (a) NTR7410, (b) NTR7450, and (c) ES20. Black circles and black triangles indicate permeate flux and humic acid concentration, respectively. Dotted lines indicate the calculated value if recovery yield = 100%.

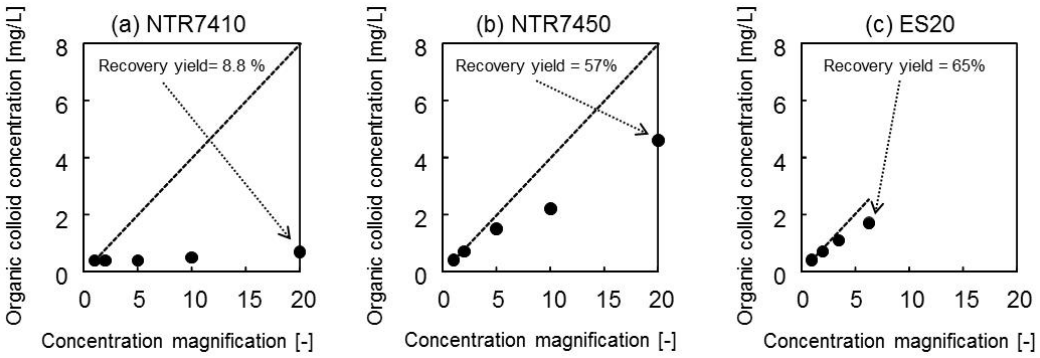

Fig. 5. Relationship between the organic colloid concentration in the concentrated solution and the concentration magnification of (a) NTR7410, (b) NTR7450, and (c) ES20. Dotted lines indicate the calculated value if recovery yield = 100%.

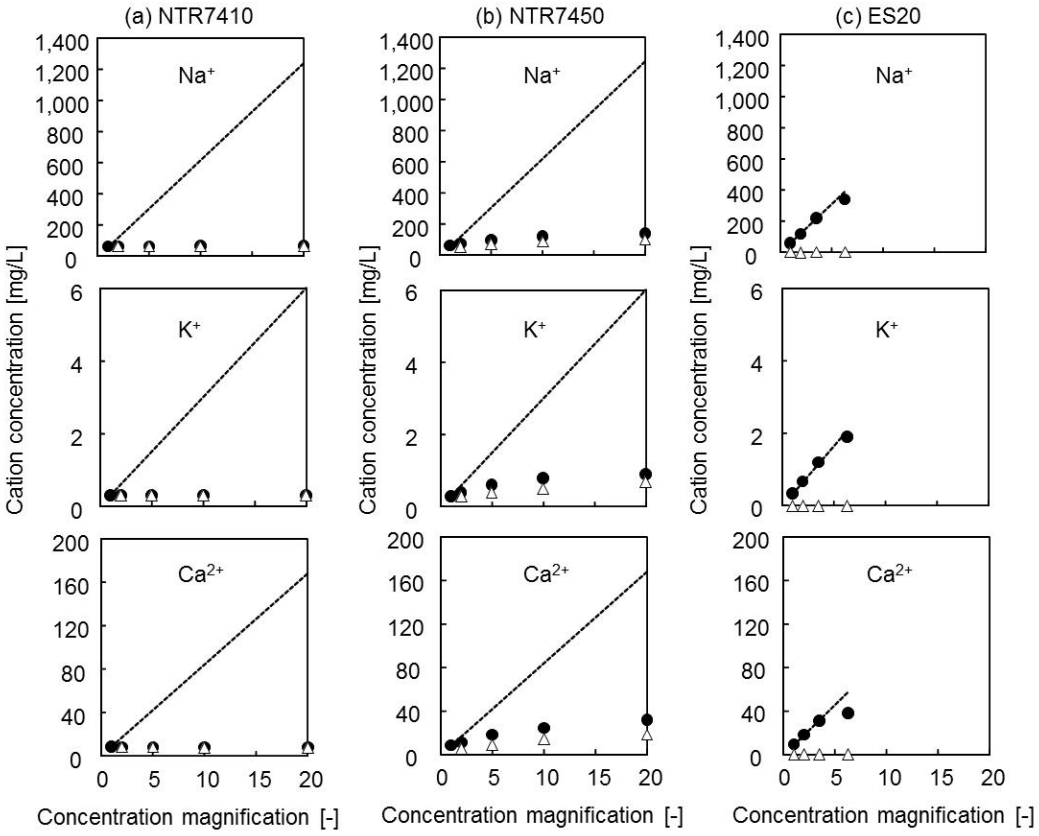

Fig. 6. Relationship between the cation concentrations in both the concentrated and permeate solutions from groundwater and the concentration magnification in the concentration tests using (a) NTR7410, (b) NTR7450, and (c) ES20. Black circles and white triangles indicate the concentration in the concentrate and permeate, respectively. Dotted lines indicate the calculated value if recovery yield = 100%.

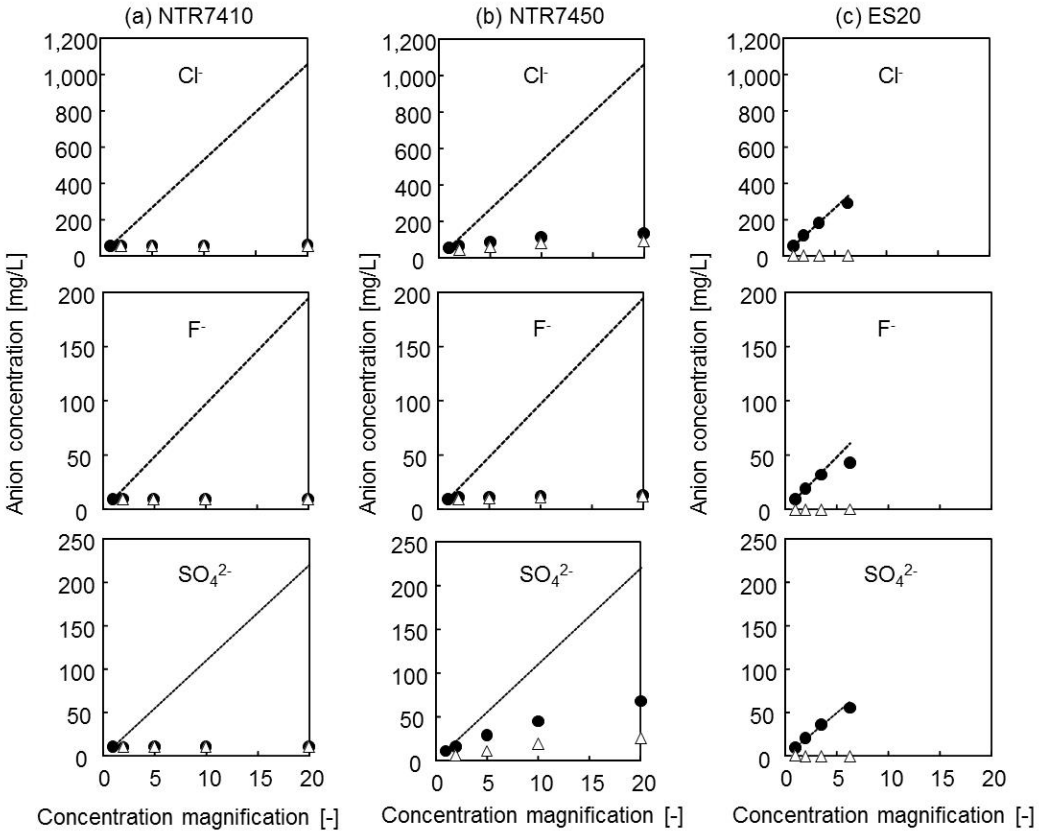

Fig. 7. Relationship between the anion concentrations in both the concentrated and permeate solutions from groundwater and the concentration magnification in the concentration tests using (a) NTR7410, (b) NTR7450, and (c) ES20. Black circles and white triangles indicate the concentration of the concentrate and permeate, respectively. Dotted lines indicate the calculated value if recovery yield = 100%.

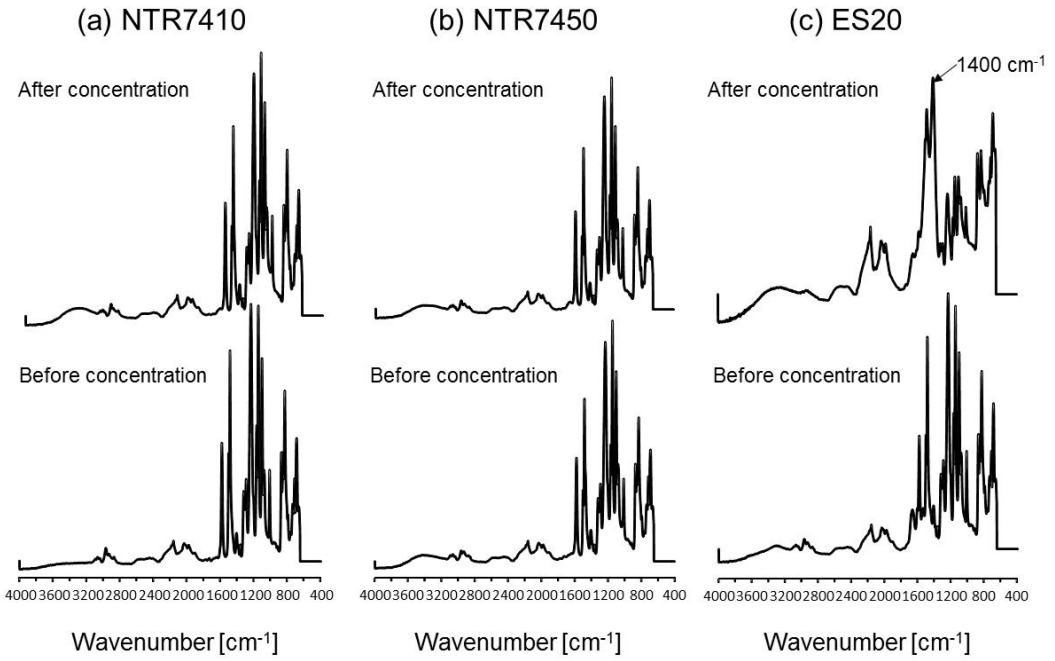

Fig. 8. FTIR spectra of the membrane surfaces after the concentration tests of groundwater using (a) NTR 7410, (b) NTR7450, and (c) ES20.

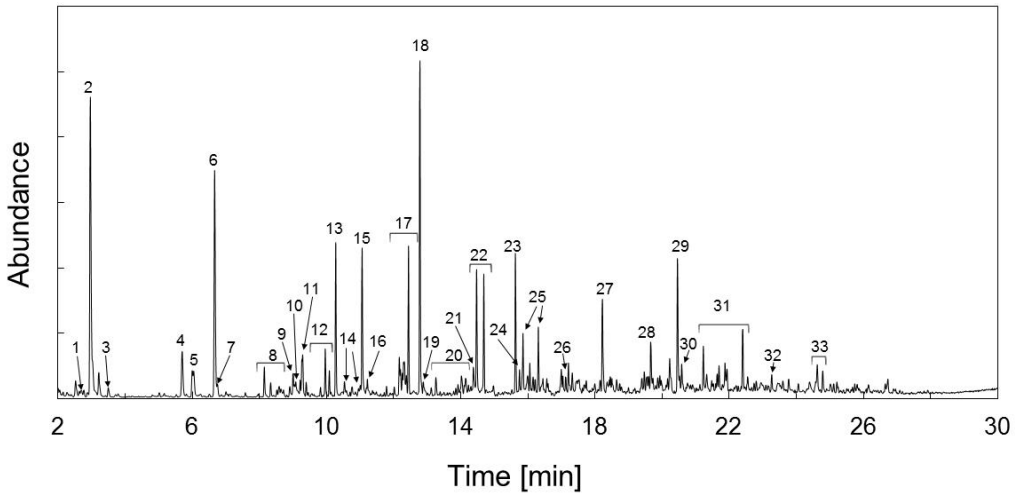

Fig. 9. Py-GC/MS pyrogram of organic colloids in groundwater concentrated by NTR7450. Peak numbers are shown in Table 2.